Predator−Prey-like Behavior of the Condensation Process in Two-Dimensional Adsorbate Systems

L. Pohlmann,[†] C. Donner,*[,‡] and H. Baumgärtel[‡]

Hahn-Meitner Institute, Glienicker Strasse 100, 14109 Berlin, Germany, and Department of Physical and Theoretical Chemistry, Free University of Berlin, Takustrasse 3, 14195 Berlin, Germany

Received: February 12, 1997; In Final Form: May 28, 1997[⊗]

Two-dimensional nonfaradaic phase transitions on solid electrodes proceed via nucleation and growth processes. Because of couplings and mutual influences of the condensation process at the surface by the adsorption process of the expanded phase from the bulk to the surface, the modeling of the nucleation and growth process presents a self-consistent problem. An alternative way to solve this problem consists of iterated differentiations of the convolution integral describing the phase transition processes. Together with the balance equation for the expanded phase one gets a closed system of four differential equations, which can be solved numerically for given initial conditions. On the basis of numerical simulations the role of the double-layer charging on the shape of current−time transients is discussed. These predictions are proofed by experimental data, measured in the system thymine/H_2O/0.X M $NaCl0_4$.

1. Introduction

Adsorption phenomena and two-dimensional phase transitions follow different mechanisms on mercury and solid electrodes in various systems. Generally one can distinguish between faradaic and nonfaradaic processes leading to phase transitions. Several classes of substances, such as DNA bases and their derivates, coumarine, lipids, and isoquinoline,[1] can undergo nonfaradaic condensation processes on mercury electrodes. At solid electrodes, especially at gold single-crystal electrodes, condensation processes were identified for some DNA bases, e.g. thymine and uracil, and coumarine. To the class of faradaic phase transitions belongs the underpotential deposition of metals on solid electrodes[2] and the anodic film formation on mercury electrodes.[3]

A common characteristic for all these first-order phase transitions is their kinetics, which includes nucleation and growth processes and which necessarily needs supersaturation. Because the electrode surface is an open system in the thermodynamic sense, the whole kinetic transition represents a nonseparable coupled system of adsorption of molecules from the solution to the surface and the real condensation process itself.[4]

For the first time Staikov[5] et al. recognized the role of adsorption in the two-dimensional phase formation process. They proposed an adsorption−nucleation-based model for describing the current−time transients, where the concentration of the expanded "gaslike" phase tends toward their potential-dependent equilibrium value and cannot be influenced by the growing islands of condensed molecules.

More developed adsorption−nucleation-based models differentiate formally between processes on energetically uniform[6] and energetically nonuniform[7] surfaces, but these models and their application to kinetic measurements[8] suffer from the neglect of adsorption as the source of the supersaturation on the surfaces.

The coupling of adsorption and condensation processes generates a time-dependent concentration of the expanded phase due to the increase of the number of noncondensed molecules by adsorption on one hand and the consumption of these molecules by growing islands of the condensed phase on the other hand. This time-dependent concentration influences the nucleation rate as well as the growth rate. For the first time it was modeled and successfully applied for the description of nonfaradaic phase formation processes on mercury in refs 9 and 10. In these models the role of adsorption kinetics was considered implicitely by a time-dependent nucleation and growth rate. This method of approximation was legitimate, because the initial time, during which the concentration of noncondensed molecules increases rapidly, was beyond the time resolution of the capacity−time measurements performed at the mercury electrode. Therefore the available capacity−time curves can only approximately represent the nucleation and growth processes.

However, chronocoulometric methods permit the detection of kinetic transients with a higher time resolution. Hence it follows that the behavior of the system in the initial time of the process, where only adsorption up to a critical nucleation concentration takes place at the surface, can be measured too. Consequently the increased time resolution in contrast to capacity methods demands a model that considers the interaction between the adsorption of the expanded phase and the condensed phase and that describes the adsorption kinetics explicitly.

Independent from the possibility of parallel reaction paths (for example for adsorption without condensation processes at special surface domains) on heterogeneous surfaces, the real two-dimensional phase transition presupposes an adsorption process that occurs at the same surface domains at which condensation takes place.

In this paper a new method will be introduced that allows the simulation of this interaction of the adsorption, nucleation, and growth processes. In the context of this model the ascending and descending parts of the experimentally obtained current−time transients are explained consistently without using additional assumptions.

It will be shown that the form of the current−time transients depends sensibly on the ratio of the rates of adsorption, nucleation, and growth.

* Corresponding author.
[†] Hahn-Meitner Institute.
[‡] Free University of Berlin.
[⊗] Abstract published in *Advance ACS Abstracts,* November 1, 1997.

S1089-5647(97)00540-3 CCC: $14.00

2. Theory

As stated above, the supersaturation of the expanded "gaslike" two-dimensional phase of adsorbed molecules is necessary as a thermodynamic driving force to generate a genuine two-dimensional condensation process. As a rule, simultaneously the corresponding bulk solution has to be undersaturated to avoid the occurrence of an additional three-dimensional condensation processes under nonfaradaic adsorption conditions.

According to this assumption the following processes can take place at the surface:

(i) The first is adsorption and desorption of the molecules from the bulk solution leading to an increase of the surface concentration of the expanded phase toward the equilibrium concentration Γ_{eq}.

(ii) After exceeding the saturation concentration, Γ_{sat}, a two-dimensional condensation via nucleation and growth processes will occur. It follows from i that the saturation concentration, Γ_{sat}, has to be lower than the equilibrium concentration, Γ_{eq}, to allow condensation processes.

(iii) Beginning with the occurrence of the first nuclei, a competitive process begins to control the concentration $\Gamma(t)$ of the expanded adsorbed phase: On one hand, the adsorbed molecules will be consumed by the growing nuclei; on the other hand the adsorption from the bulk solution tends to compensate this loss of molecules. Further, this time-dependent concentration $\Gamma(t)$ of the expanded phase itself controls the running processes of subsequent nucleation and growth.

(iv) This process will be stopped when the whole surface (or, in the case of an inhomogeneous surface, all the domains of the surface at which condensation can take place) is covered by the condensed phase. Mathematically this process is described to a good approximation by the so-called Avrami theorem.[11,12]

To illustrate the special kind of coupling and mutual influences controlling the nucleation and growth processes by means of the concentration of the expanded phase, it can be useful to stress its analogy to the interaction of a predator with a prey in population dynamics. Here, the prey, e.g. "hares" (the adsorbed molecules in the expanded phase) feeding on the growing "grass" (the adsorption from the bulk solution) is on one hand proliferating but on the other hand will be "eaten" by the predator, e.g. by "foxes" (the growing nuclei of the condensed phase), which are also proliferating if the there are enough "hares" around. In this way the population density of the "hares" depends on the balance of growing "grass" and the consumption by the proliferating "foxes". On the contrary, the further proliferation of "foxes" depends sensitively on the population density of the "hares".

Mathematical modeling of the above decribed processes affords at least three equations:

(1) A differential equation describing the balance of the expanded phase $\Gamma(t)$. (Note: All concentrations used in the model of this paper are surface concentrations.) This equation can be easily derived by the calculation of, on one hand, the net number of molecules (measured in moles) M that are gained by the free surface per unit time due to the adsorption kinetics,

$$\left(\frac{dM}{dt}\right)_{gain} = k_a(\Gamma_{eq} - \Gamma)S_{free}$$

(with k_a the adsorption rate constant, Γ_{eq} the equilibrium concentration of noncondensed molecules, and S_{free} the area of surface not yet covered by the condensed phase), and, on the other hand, by subtracting the number of molecules that are lost per unit time due to the incorporation into the growing nuclei of the condensed phase:

$$\left(\frac{dM}{dt}\right)_{loss} = \Gamma_{film}\frac{dS}{dt} = \Gamma_{film}\frac{S_{free}}{S_E}\frac{dS_{ext}}{dt}$$

$$\frac{dS_{ext}}{dt} = 2\pi R\frac{dr}{dt} = 2\pi R k_w(\Gamma - \Gamma_{sat})$$

(with Γ_{film} the surface concentration of the condensed phase, S_E the surface area of the electrode, S the real surface area of the film-covered surface, $S = S_E - S_{free}$, S_{ext} the extended surface area of the film, not accounting for overlap, R the sum of radii of all nuclei, dr/dt = linear growth rate of one nucleus, and Γ_{sat} the saturation concentration). The difference of both contributing terms then has to be divided by the free surface area in order to obtain the changes in the concentration Γ of the expanded phase. This leads finally to the balance equation:

$$\frac{d\Gamma}{dt} = \left[\left(\frac{dM}{dt}\right)_{gain} - \left(\frac{dM}{dt}\right)_{loss}\right]/S_{free} = k_a(\Gamma_{eq} - \Gamma) - \Gamma_{film}pk_w(\Gamma - \Gamma_{sat}) \quad (1)$$

with $p = 2\pi R/S_E$ the total periphery length of all nuclei per unit surface.

(2) An integral equation describing the nucleation and growth of the condensed phase without the overlap of the growing nuclei, leading to the so-called "extended" coverage of the surface,

$$\Theta_{ext} = \int_0^t j_n(t')\pi r^2(t,t')\,dt' \quad (2)$$

with j_n the nucleation rate per unit surface, $r(t,t')$ the actual radius of a nucleus that occurred at time t', and $\Theta_{ext} = S_{ext}/S_E$ the extended coverage of the surface by the condensed phase.

(3) The Avrami theorem connecting the extended coverage $\Theta_{ext}(t)$ with the real coverage $\Theta(t)$:

$$\Theta = 1 - \exp(\Theta_{ext}) \quad (3)$$

At this stage of modeling the coupling of the eqs 1 and 2 occurs only in a hidden way, whereas the time dependence of the nucleation rate and the growth of nuclei in the integral (2) could be obtained through their concentration dependencies (see below); the calculation of the concentration−time dependence itself by means of eq 1 requires the knowledge of the total periphery length of all nuclei, which is not explicitly given in eq 2. One way to tackle this problem consists of iterated differentiations of the integral eq 2 leading to a system of differential equations. For this reason it is useful to restrict our model to the case where the nucleation rate and the growth of the nuclei as well are completely defined by the actual (time-dependent) concentration of the expanded phase:

$$j_n(t) = j_n(\Gamma(t)), \quad r(t,t') = \int_{t'}^t k_w(\Gamma(t'') - \Gamma_{sat})\,dt'' \quad (4)$$

where k_w is rate constant of linear growth according to eq 1.

This assumption is in many cases close to the real situation, but it should be noted that it excludes some secondary effects such as Ostwald ripening. Furthermore, effects of surface diffusion also would violate the conditions under which eqs 4 are valid. For this reason in the following it will be assumed that the surface diffusion is sufficiently fast to avoid spatial inhomogeneities of the surface concentration $\Gamma(t)$. Using eqs

4, the iterated differentation of the integral (2) leads to a finite system of differential equations. The first differentiation yields

$$\frac{d\Theta_{ext}}{dt} = j_n(t)\pi r_0^2 + k_w(\Gamma - \Gamma_{sat})\int_0^t j_n(t')2\pi r(t,t')\,dt' \quad (5)$$

Furthermore it was assumed that the initial radius r_0 of the occurring nuclei can be neglected; that is, the first term on the right-hand side of eq 5 can be omitted. The remaining integral in eq 5 represents the total periphery length p of all nuclei per unit surface needed for the coupling with eq 1:

$$p = \int_0^t j_n(t')2\pi r(t,t')\,dt' \quad (6)$$

The insertion of eq 6 into eq 5 transforms the integrodifferential equation into a differential equation for the extended surface coverage:

$$\frac{d\Theta_{ext}}{dt} = k_w(\Gamma - \Gamma_{sat})p \quad (7)$$

Subsequent differentiation of eq 6 leads in an analogous manner to the differential equations for the total periphery length per unit surface,

$$\frac{dp}{dt} = 2\pi k_w(\Gamma - \Gamma_{sat})\, n(t) \quad (8)$$

with $\quad n(t) = \int_0^t j_n(t')\,dt'$

and finally for the surface density of nuclei $n(t)$:

$$\frac{dn}{dt} = j_n(\Gamma(t)) \quad (9)$$

Here, the nucleation rate will be assumed to follow the Volmer−Zeldovich law[16] for homogeneous two-dimensional nucleation:

$$j_n = k_n Z\Gamma^2(t)\exp\left(\frac{K}{\ln(\Gamma(t)/\Gamma_{sat})}\right) \quad (10)$$

Here is k_n the preexponential factor of the rate constant of nucleation, Z is the so-called Zeldovich factor accounting for nonequilibrium effects, and the exponent depends on the free enthalpy of nucleation. In the two-dimensional case K means

$$K = \pi\epsilon^2 A/(kT)^2$$

where ϵ is the line tension of the condensed phase, A is the area of a molecule in the condensed phase, T is the temperature, and k is the Boltzmann constant.

Finally the differentiation of the Avrami theorem (3) and insertion of eq 7 lead to

$$\frac{d\Theta}{dt} = k_w(\Gamma - \Gamma_{sat})(1 - \Theta)p \quad (11)$$

The differential equations (1), (8), (9), and (11) form a closed system of nonlinear equations describing the processes i−iv and their mutual couplings in a very lucid manner. Due to its nonlinearity, the system can only be solved numerically for given initial conditions. For comparison with the experimental results it is reasonable to choose the following initial conditions:

(1) The initial surface adsorbate concentration Γ_0 should be below the saturation concentration Γ_{sat}:

$$\Gamma(0) = \Gamma_0 < \Gamma_{sat}$$

(2) The initial number of nuclei n should be zero, if preclustering effects or heterogeneous nuclei are excluded:

$$n(0) = 0$$

(3) Obviously under these conditions the initial total periphery length p and the surface area covered by nuclei must be zero:

$$p(0) = 0,\ \Theta = 0$$

If athermal preclusters can affect the nucleation process, one should use a different initial condition for the density of nuclei $n(0) > 0$, as will be shown in a forthcoming paper.[17]

The solution of the system of differential equations described above depends on seven parameters: on the rate constants of adsorption k_a, linear growth k_w, and nucleation k_n, on the equilibrium concentration Γ_{eq} and the saturation concentration Γ_{sat}, on the two-dimensional density of the condensed phase Γ_{film}, and on the effective free energy of nucleation K.

To analyze the dependence of the numerical solutions on the parameter values, it is convenient to reduce the number of independent parameters by the introduction of dimensionless variables: Using this method the new units of the dependent and independent variables are constructed as combinations of the given system parameters. Of course, there are several parameter combinations possible to obtain the same unit. The choice used here followed from the consideration that the variation of the measurement potential should affect only two of the new dimensionless parameters (namely α and γ). The new units are

concentration unit $\quad \Gamma_{film}$

time unit $\quad t_{unit} = 1/\sqrt[3]{k_n k_w^2 \Gamma_{film}^4}$

length unit $\quad l_{unit} = \sqrt[3]{k_w/k_n\Gamma_{film}}$

Using these new units, the dependent and independent variables of the system are transformed to new dimensionless variables (the coverage Θ is dimensionless by definition):

$$t_{dl} = t/t_{unit};\quad c_a = \Gamma/\Gamma_{film};\quad p_{dl} = pl_{unit};\quad n_{dl} = n(l_{unit})^2$$

Expressed in these new variables, the system of differential equations (1, 8, 9, 11) is transformed into

$$\frac{dc_a}{dt_{dl}} = \alpha(\gamma - c_a) - (c_a - \delta)p_{dl} \quad (13)$$

for the concentration of adsorbed molecules;

$$\frac{d\Theta}{dt_{dl}} = (1 - \Theta)(c_a - \delta)p_{dl} \quad (14)$$

for the surface coverage of the condensed phase;

$$\frac{dp_{dl}}{dt_{dl}} = 2\pi(c_a - \delta)n_{dl} \quad (15)$$

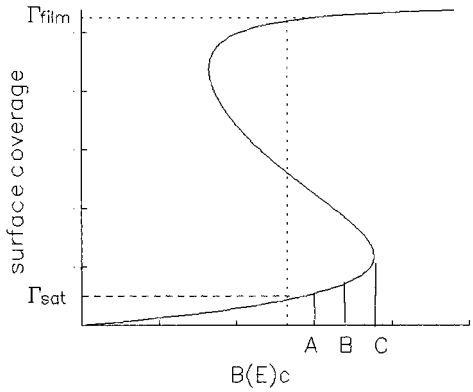

Figure 1. Schematic representation of the Frumkin isotherm and the considered potential regions A, B, and C belonging to the different concentrations of adsorbed molecules.

for the total periphery length; and

$$\frac{dn_{dl}}{dt_{dl}} = c_a^2 Z \exp\left(-K/\ln\left(\frac{c_a}{\delta}\right)\right), \quad c_a > \delta \tag{16}$$

for the density of nuclei.

The new dimensionless parameters are now

K	unchanged constant of the Volmer-Zeldovich law (10)
$\alpha = \dfrac{k_a}{\sqrt[3]{k_n k_w^2 \Gamma_{film}^4}}$	dimensionless combination of rate constants, depending on the applied potential through k_a
$\gamma = \Gamma_{eq}/\Gamma_{film}$	dimensionless equilibrium concentration, depending on the applied potential through Γ_{eq}
$\delta = \Gamma_{sat}/\Gamma_{film}$	dimensionless saturation concentration

In this way the number of independent parameters, which have to be varied in the numerical simulations, was reduced from seven to four.

3. Numerical Simulations

For the numerical simulations it is reasonable to take parameter values typical for situations in real systems. There are only a few papers, to our knowledge, in which the experimental data were analyzed with consideration of the time dependence of the surface concentration $\Gamma(t)$ of noncondensed molecules.[9,10] In these papers the time dependence of noncondensed molecules was approximated by stepwise defined functions using averaged concentrations and, as a result, averaged nucleation and growth rates. Parameter values[10] obtained in this way can be used as a basis for the following simulations.

To interpret the parameter values in terms of the model presented here, it is necessary to correlate the variations in the final measuring potential with variations in the equilibrium concentration of adsorbed molecules Γ_{eq}. For a first approximation this can be done using the Frumkin isotherm (Figure 1):

$$Bc = \frac{\theta}{1-\theta}\exp(-a\theta) \tag{17}$$

where θ is the coverage of adsorbed molecules (in the expanded, "gaslike" state), a is the interaction coefficient, and c is the bulk concentration of the molecules. The adsorption constant B is dependent in the case of adsorption of neutral molecules on the applied potential in the following way:

$$B(E) = B_0 \exp(-\beta(E - E_m)^2) \tag{18}$$

with B_0 and β being some positive constants.

Three different potential regions were taken representing different equilibrium concentrations and therefore different supersaturation conditions: (A) low supersaturation; (B) high supersaturation; and (C) supersaturation at the boundary of the metastable region.

Following these considerations three typical parameter regions were obtained listed in Table 1.

A typical simulation of the system (13−16) for medium values of the interval A is shown in Figure 2. The differential equations were solved using an adaptive Runge−Kutta method of fourth order. The shape of the concentration curve of the noncondensed molecules c_a shows a clear maximum followed by an asymptotic approach of the saturation concentration, as predicted in ref 13. It should be noted that the continuous increase of the periphery length p, even if the surface coverage reached its maximum, is due to the fact that p here represents the "extended" periphery length in terms of the Avrami theorem, whereas the coverage is already the corrected real surface coverage.

In Figures 3 and 4 three different scenarios are shown corresponding to medium values of the regions A, B, and C. Increasing supersaturation increases the maximum value of the concentration of noncondensed molecules (Figure 3). As a result, the density of nuclei also increases (Figure 4), leading in turn to a steeper descent of the concentration after reaching the maximum value (Figure 3).

The functional relations between the fundamental variables, as shown in Figures 2−4, determine the nucleation and growth process at electrodes. But the only measurable quantity in kinetic investigations is the current−time behavior of the system after a single potential step from outside into the condensation region. As long as faradaic processes are excluded, the measured current signal represents at every time the actual adsorption kinetics. This means, from the microscopic point of view, that every molecule adsorbed at the electrode contributes the same change of charge to the whole process, independent of the particular state of the molecules at the electrode. This is valid in the approximation of the Frumkin model of the two parallel plate condensers.[14] In this model, to each adsorbed molecule a specific capacity C_a (per unit surface) is attributed, which is, as a rule, smaller than the specific capacity of the adsorbate free surface C_0. Consequently the actual current density i must be proportional to the net adsorption flux (first term in eq 1) at the island-free part of the surface:

$$i = (1 - \Theta)(C_0 - C_a)Ek_a(\Gamma_{eq} - \Gamma)/\Gamma_{film} \tag{19}$$

or, in dimensionless form,

$$i_{dl} = (1 - \Theta)(\gamma - c_a)$$

with the current density unit $\quad i_{unit} = (C_0 - C_a)Ek_a \quad (20)$

In Figure 5 are shown some typical current−time transients for phase transition processes, obtained from the numerical simulations according to the presented model. The first descending part of the transients immediately after time $t = 0$ desribes the adsorption kinetics up to a limiting value, where the first nuclei are born at the surface. With increasing consumption of adsorbed molecules by growing islands, the

TABLE 1: Parameter Variations for Numerical Simuations in Different Potential Regions[a]

	region A			region B			region C		
Γ_{eq} 10^{10}/mol cm^{-2}:	1.4	1.4	1.4	1.8	1.8	1.8	2.2	2.2	2.2
γ	0.233	0.233	0.233	0.300	0.300	0.300	0.366	0.366	0.366
α	0.16	0.13	0.10	0.12	0.10	0.08	0.09	0.07	0.05

[a] K: 0.076. Γ_s: 1×10^{10} mol cm^{-2}. k_a: 1 s^{-1}. Γ_{film}: 6×10^{10} mol cm^{-2}. δ: 0.166.

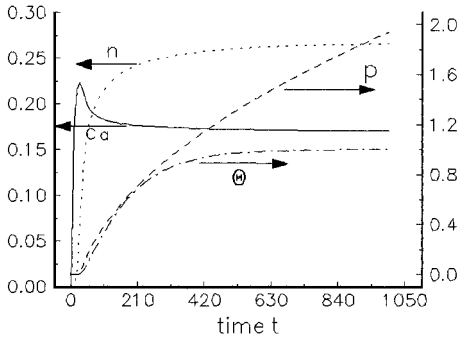

Figure 2. Simulated time behavior of the dimensionless variables: (—) concentration of adsorbed molecules c_a; (•••) density of nuclei n; (—•—) surface coverage of condensed islands Θ; (— — —) total periphery length per surface area p for $\gamma = 0.300$, $\alpha = 0.08$.

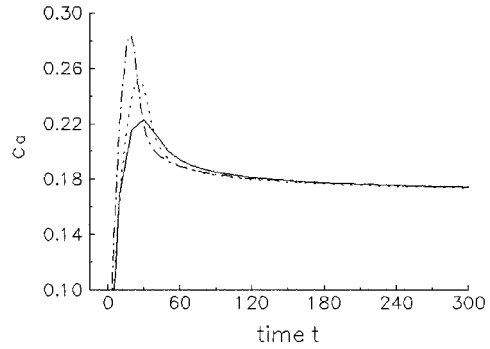

Figure 3. Concentration−time behavior of adsorbed noncondensed molecules for different dimensionless parameters: (—) $\gamma = 0.233$, $\alpha = 0.13$; (•••) $\gamma = 0.300$, $\alpha = 0.08$; (—•—) $\gamma = 0.366$, $\alpha = 0.05$.

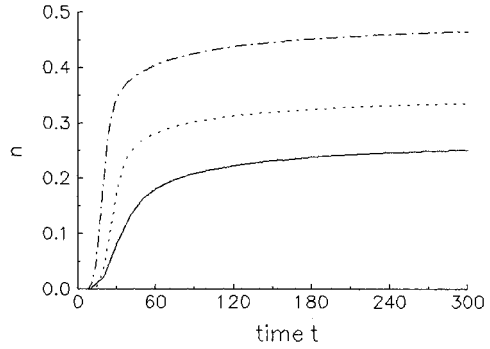

Figure 4. Density of nuclei for the same simulations shown in Figure 3.

adsorbed molecules at the island-free surface will be depleted and therefore the adsorption current must increase again up to a maximum. The second descending part of the current is caused by the shrinking area of the free surface.

These simulated curves allow a deeper understanding of experimentally obtained current-time transients (as shown in Figures 8 and 9).

The maximum in the current−time transients is sharper the greater the difference between the densities of the condensed and noncondensed phases is. In turn from this follows that the maximum will be vanishing if these two densities become nearly equal. This is the case for systems close to the critical

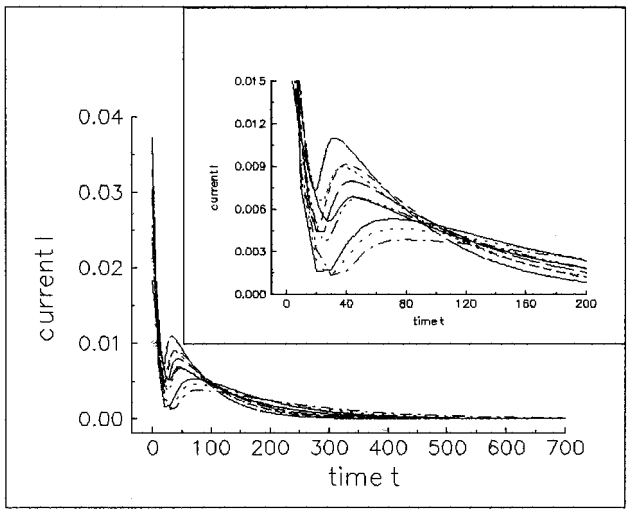

Figure 5. Current−time transients followed from simulations done with parameter sets listed in Table 1.

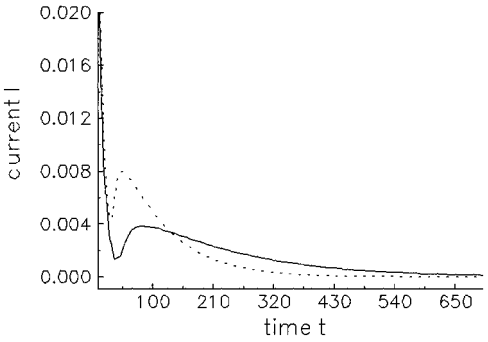

Figure 6. Current−time transients for different values of supersaturation: (—) $\alpha = 0.10$, $\gamma = 0.23$; (•••) $\alpha = 0.10$, $\gamma = 0.300$.

temperature of the phase transition. This means that the maximum in the current−time transients is a sufficient but not a necessary condition for two-dimensional phase transitions.

The effect of the variation of the bulk concentration c on current−time transients is demonstrated in Figure 6 due to the variation of the equilibrium concentration γ by keeping all other parameters constant. As expected, the higher maximum value corresponds to the higher bulk concentration. In this case the overall condensation kinetics is much faster as a result of the higher nucleation density (see also Figure 4). A similar effect would occur if the potential dependence of the equilibrium constant $B(E)$ is dominated by the potential dependence of the desorption constant.

Another effect on the current−time transients, which has to be discussed here, is the charging (or discharging) of the electrode double layer. If the time constant of the adsorption process becomes of the same order as the time constant of the double-layer charging, it is not possible to separate both processes. The occasionally practiced method of formally subtracting the double-layer discharging measured separately in an adsorbant-free solution from the curves corresponding to the phase transition is not quite correct because even the electrode potential itself is changing during the charging process.

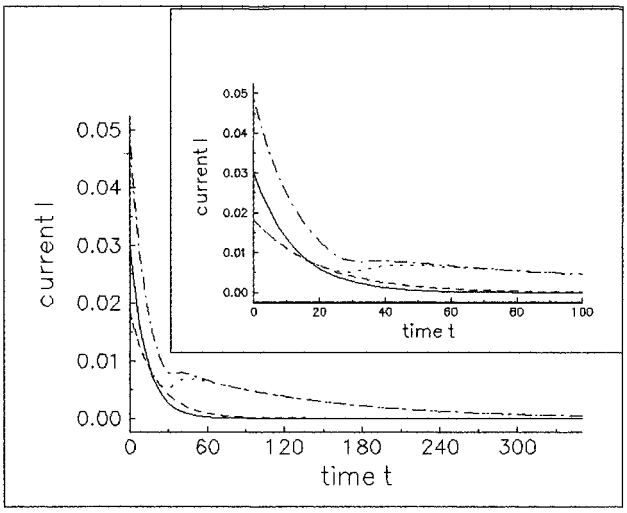

Figure 7. (···) Simulated current−time transient for $\alpha = 0.05$, $\gamma = 0.366$; (—) double layer charging; (—·—) current time transients plus double-layer charging; (— — —) adsorption current alone.

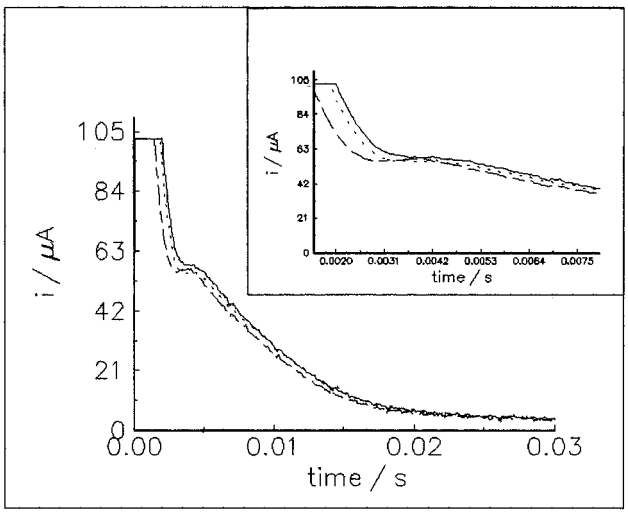

Figure 8. Experimental current−time transients measured in the system 12 mmol thymine/0.1 M $NaClO_4$ on Au(111) ∅ 5 mm by single potential step methods. $T = 20$ °C. Measuring potential = 0.74 mV. Start potentials: (—) −0.83 mV; (···) −0.82 mV; (— — —) −0.80 mV.

This method can only be applied if the adsorption rate is much slower (or much faster) than the double-layer charging rate.

The influence of the charging process can easily be simulated in the frame of the model presented here by the addition of exponential charging curves to the simulated current−time transients. As is shown in Figure 7, in this way the minimum between the well-separated parts of the transients (adsorption and condensation) will become shallower and can even disappear. Experimentally this effect can be traced by the variation of the ion strength of the solution as well as by changing the difference between the prepolarization potential and the measuring potential. Both effects are shown in Figures 8 and 9 for the case of the condensation of thymine (12 mmol) on Au(111).

Another point to be discussed here is the interpretation and the handling of the exponential decaying part of the current−time transients, supposing that the double-layer discharging can here be neglected for reasons discussed above. The usual practice is based on the assumption that the adsorption and the condensation processes are independent from each other.[7,8] This assumption can be justified when pure adsorption (without condensation) takes place on one kind of domain of a polycrystalline surface, whereas pure condensation occurs on surface domains with other physical properties.

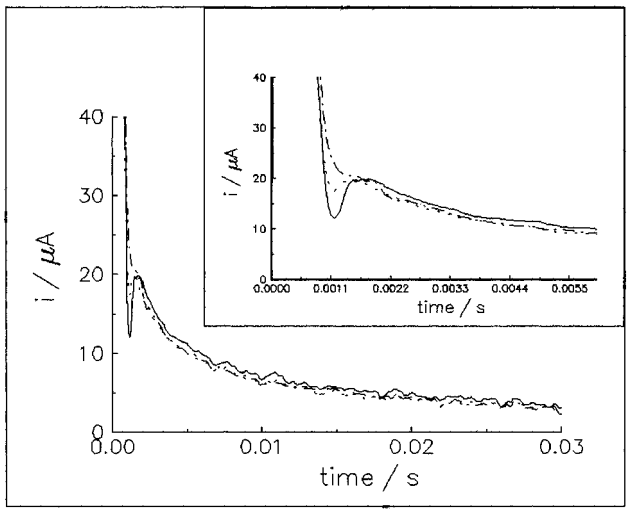

Figure 9. Experimental current−time transients measured in the system 12 mmol thymine /0.5 M $NaClO_4$ on Au(111) ∅ 5 mm by single potential step methods. $T = 20$ °C. Measuring potential = −0.71 mV. Start potentials: (—) −0.75 mV; (···) −0.80 mV; (— — —) −0.95 mV.

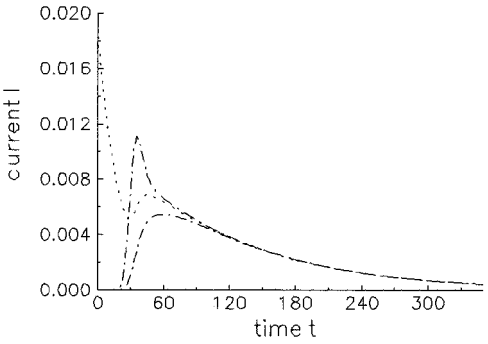

Figure 10. (—) Simulated current−time transient for $\alpha = 0.05$, $\gamma = 0.366$; (···) difference between the current−time transient and the adsorption current alone; (—·—) growth of film coverage derived from the coverage−time dependence.

The whole problem was discussed in a lucid way by Bosco and Rangarajan.[6,15] In these papers the authors distinguish three possible reaction processes: (a) phase growth via direct incorporation from bulk solution and independent adsorption on the free surface, (b) adsorption and subsequent growth via adatom incorporation, and (c) a combination of a and b. The reaction process a, which was modeled in refs 6 and 15, is not very probable in nonfaradaic two-dimensional phase transitions (with undersaturated bulk concentrations), where the supersaturation occurs only in the adsorbed phase. A formal application of model a to this kind of process would lead to a seeming shift of the nucleation and growth process at the time axis (see below). On the other hand the reaction mechanism b, which has not been outlined in detail by the authors, is more appropriate for the description of nonfaradaic phase transitions where the growth of the nuclei is mainly due to the already adsorbed molecules. The model presented in the present paper outlines, under some restrictions, the Bosco and Rangarajan model b.

The effect of both treatments of the adsorption process can be easily demonstrated using the model of this paper: In Figure 10 three curves are shown, the first one obtained by a solution of the model presented here and the second one generated from the first by subtracting the current−time transient referring to an adsorption kinetics, which is not influenced by any other processes.

The usual way is to interpret this second curve as a description of the growth of islands alone. Then, the integration of this

curve would lead to the true coverage−time dependence of the growing film. Unfortunately this interpretation is not quite correct. This can be easily shown with the third curve in Figure 10, which represents the growth of the film coverage derived from the coverage−time dependence obtained by solving the model system for the same set of parameter values. It turns out that both curves are quite different. This quantitative and qualitative difference comes from the fact that in reality the adsorption process (at the film-free surface) is not independent from the film growth, because the rapid depletion of adsorbed molecules leads to an acceleration of the adsorption rate. Therefore the above described way of interpretation of the experimental data can only be understood as a very rough approximation, which neglects the interaction of the adsoption and the growth processes. A more consistent way would be the nonlinear curve fitting to the differential equation system representing the model described here.

4. Conclusions

In the presented model it was shown that the simultaneous consideration of the complex condensation processes consisting of nucleation, growth, and adsorption was necessary for describing the kinetics of phase transitions. This problem was already discussed by Bosco and Rangarajan.[6,15] It appears that the reaction mechanism b, which has not been outlined mathematically by these authors, is more appropriate for the description of nonfaradaic phase transitions. The model presented here intends to bridge this gap for the special case of kinetics-determined island growth. It is able to describe in a consistent way the interplay of adsorption, nucleation, and growth. It illustrates the influence of the potential and the bulk concentration on this interplay which leads to the experimentally observable current−time transients.

References and Notes

(1) Buess-Herman, Cl. *Prog. Surf. Sci*. **1994**, *4*, 335.
(2) Kolb, D. M. *Advances in Electrochemistry and Electrochemical Engineering*; Gerischer, H., Tobias, C. W., Eds.; Wiley-Interscience: New York, 1978; Vol. 11, p 125.
(3) Philipp, R.; Retter, U. *Thin Solid Films* **1992**, *207*, 42.
(4) Jüttner, K.; Staikov, G.; Lorenz, W. J.; Schmidt, E. *J. Electroanal. Chem*. **1977**, *80*, 67.
(5) Staikov, G.; Jüttner, K.; Lorenz, W. J.; Schmidt, E. *Electrochim. Acta* **1978**, *23*, 305.
(6) Bosco, E.; Rangarajan, S. K. *J. Electroanal. Chem*. **1981**, *129*, 25.
(7) Hölzle, M. H.; Kolb, D. M. *Ber. Bunsen-Ges. Phys. Chem*. **1994**, *98*, 330.
(8) Hölzle, M. H.; Wandlowski, Th.; Kolb, D. M. *Surf. Sci*. **1995**, *335*, 281.
(9) Donner, C.; Pohlmann, L.; Baumgärtel, H. *Surf. Sci*. **1996**, *345*, 363.
(10) Pohlmann, L.; Donner, C.; Baumgärtel, H. *Surf. Sci.* **1996**, *359*, 280.
(11) Avrami, M. *J. Chem. Phys.* **1940**, *8*, 212.
(12) Kolmogorov, A. N. *Bull. Acad. Sci. USSR (Sci. Math. Nat.)* **1937**, *3*, 355.
(13) Donner, C.; Pohlmann, L.; Baumgärtel, H. *Ber. Bunsen-Ges. Phys. Chem.* **1996**, *100*, 1691.
(14) Gileadi, E. *Electrode Kinetics*; VCH Verlagsgesellschaft mbH: Weinheim, 1993.
(15) Bosco, E.; Rangarajan, S. K. *J. Chem. Soc., Faraday Trans. 1* **1981**, *77*, 1673.
(16) Toschev, S. In: Crystal Growth−An Introduction; Hartmann, P., Ed.; 1973; p 1.
(17) Donner, C.; Kirste, S.; Pohlmann, L.; Baumgärtel, H. *Chem. Phys. Lett.*, in press.